Notes on SRG unitary matrix factorization

R.J. Furnstahl[1,*]

[1] *Department of Physics, The Ohio State University, Columbus, OH 43210*

(Dated: November 23, 2016)

Abstract

Factorization of the SRG unitary transformation operator revisited.

* furnstahl.1@osu.edu

CONTENTS

I. OVERVIEW

In past work we looked at the factorization of the SRG unitary transformation operator. In Section II we've copied some of the results from the deuteron operator paper. We would like to extend these results and figures in light of subsequent calculations and needs.

To do list:

- Make figures for numerical tests of factorization for more partial waves, including in particular the ${}^3\mathrm{S}_1$–${}^3\mathrm{D}_1$ off-diagonal transformation.
- Make figures showing the weak k dependence at large, fixed q.
- Test whether "local decoupling" implies factorization as long as momenta differ by (sufficiently) more than λ.

II. OPERATOR FACTORIZATION (SELECTIONS FROM DEUTERON PAPER)

...We can anticipate simplifications by exploiting this separation of scales provided by the SRG; in particular, we expect a factorization of the evolved operator based on operator-product-expansion (OPE) arguments applied to nonrelativistic effective theories [1, 2].

A. Numerical Verification of Factorization

Previous calculations of the deuteron momentum distribution suggested that the unitary evolution operator, $U_\lambda(k,q)$,[1] *factorizes* into a function of k times a function of q, $U_\lambda(k,q) \to K_\lambda(k)Q_\lambda(q)$, for $k < \lambda$ and $q \gg \lambda$ [4]. To numerically test for factorization in the unitary transformation, we use transformations generated via [SRG evolution], and consider the ratio

$$\frac{U_\lambda(k_i,q)}{U_\lambda(k_0,q)} \xrightarrow{?} \frac{K_\lambda(k_i)Q_\lambda(q)}{K_\lambda(k_0)Q_\lambda(q)}\,, \tag{1}$$

[1] Because λ is an important momentum scale in our factorization discussion, we use the notation U_λ with $\lambda = s^{-1/4}$ rather than U_s in this section.

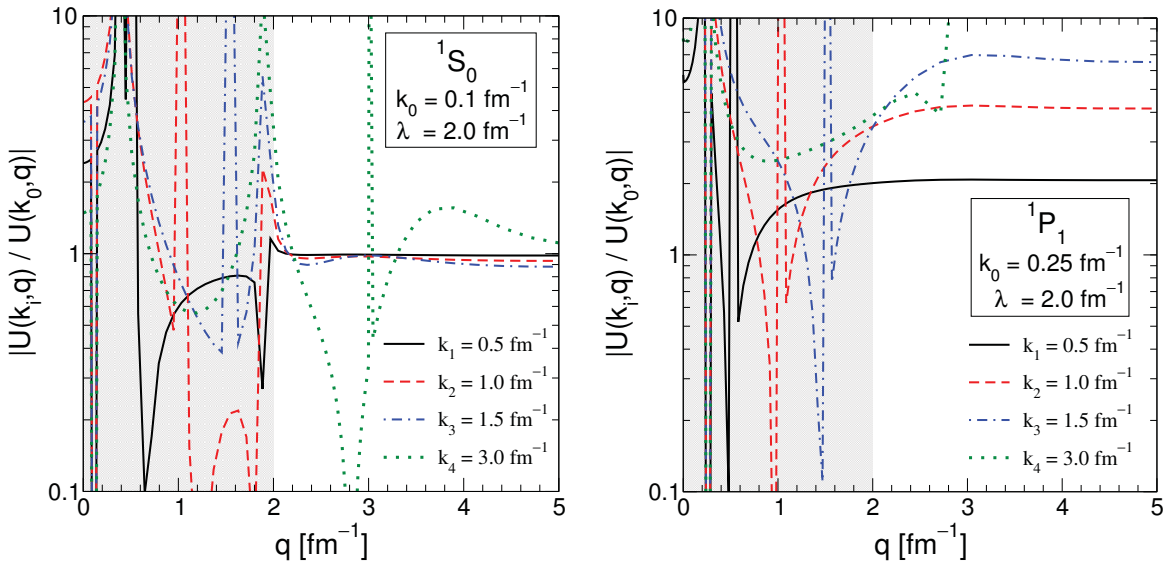

(a) (b)

FIG. 1. Numerical tests of factorization of the unitary transformation $U_\lambda(k,q)$ by plotting the ratio in Eqs. (1) and (31) as a function of q for fixed k_0 and several values of k_i. Plateaus in q indicate factorization. The unitary transformations are generated from the Argonne v_{18} (AV18) [3] potential evolved to $\lambda = 2\,\mathrm{fm}^{-1}$ in the (a) ^{1}S$_0$ and (b) ^{1}P$_1$ partial waves. The shaded region marks $q < \lambda$.

holding k_i and k_0 constant with $k_0 \ll \lambda$. If there is factorization, the q dependence should cancel; that is, for $k < \lambda$ and $q \gg \lambda$ we should find

$$\frac{U_\lambda(k_i,q)}{U_\lambda(k_0,q)} \approx \frac{K_\lambda(k_i)}{K_\lambda(k_0)} \,. \tag{2}$$

In Figs. 1 and 2 we plot the ratio in Eq. (1) versus q for representative cases. The signature of factorization is a plateau in q. The shaded regions are where $q \leq \lambda$. In all cases, there is no factorization in this region, consistent with the requirement that $q \gg \lambda$. In the unshaded region we see definite plateaus for $q > \lambda$ as long as $k_i < \lambda$, with diminishing prominence as k_i increases (they disappear for $k_i > \lambda$). Thus we have at least a qualitative verification of factorization. Note that Fig. 2(b) shows that for larger λ the clean factorization breaks down (as well as restricting the applicable domain).

The singular value decomposition (SVD) can be used as a tool to quantitatively analyze the extent to which U_λ factorizes. The SVD of a matrix M can be expressed in general as an outer product expansion

$$M = \sum_{i=1}^{r} d_i \mathbf{u}_i \mathbf{v}_i^t \,, \tag{3}$$

where r is the rank of the matrix and the d_i are the singular values (in order of decreasing value). The idea is that if the first singular value, d_1, is sufficiently large compared to the others, the first term dominates and we have a factorized approximation. We can apply this to U_λ in the region where high and low momentum couple. Thus, the vector $\mathbf{u}_1$ would correspond to the low momentum function $K_\lambda(k)$ from Eq. (1) and $\mathbf{v}_1$ to $Q_\lambda(q)$. If valid, one can calculate the factorized operator using the unitary transformation obtained directly

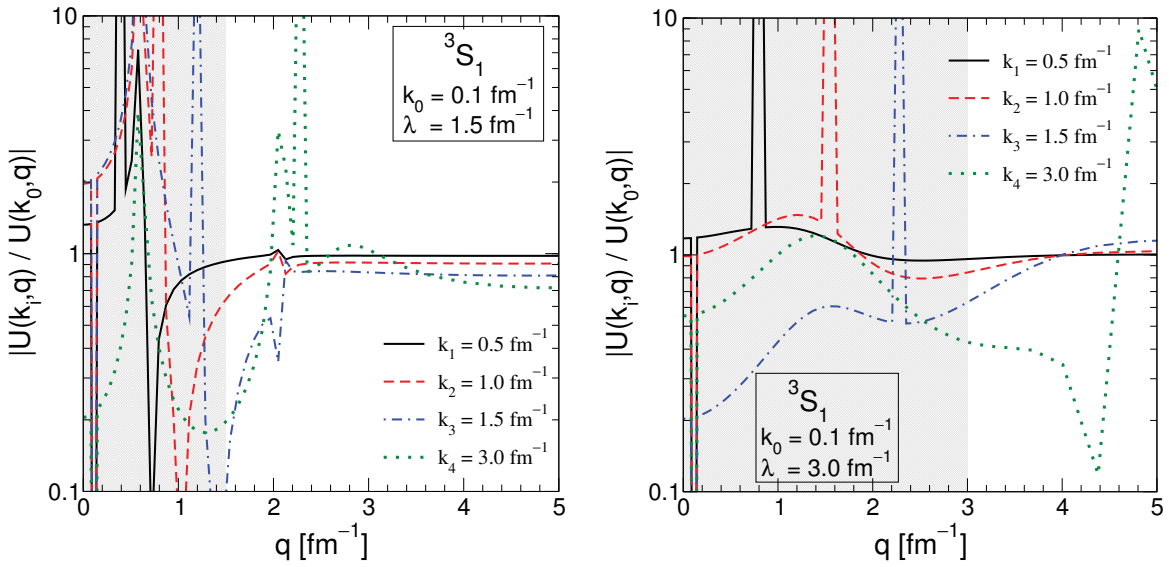

FIG. 2. Same as Fig. 1 but for the ^{3}S$_1$ partial wave and λ of (a) 1.5 fm^{-1} and (b) 3 fm^{-1}.

	^{1}S$_0$			^{3}S$_1$–^{3}D$_1$		
Potential	d_1	d_2	d_3	d_1	d_2	d_3
AV18	0.763	0.033	0.007	0.671	0.015	0.008
N3LO 500 MeV	1.423	0.221	0.015	1.873	0.225	0.044
N3LO 550/600 MeV	3.074	0.380	0.061	4.195	0.587	0.089

TABLE I. Singular values of the unitary transformation $U(k,q)$ for $q > \Lambda$ and $k < \Lambda$ (see discussion in text; units in fm^{-1}) corresponding to the given potentials at $\lambda = 2$ fm^{-1} in the ^{1}S$_0$ partial wave and ^{3}S$_1$–^{3}D$_1$ coupled channel.

from the SVD. Moreover, the expansion provided by the SVD allows us to make systematic corrections to the factorized unitary transformation and the operators evolved with it.

To test if such an expansion can be used, the first few singular values have been calculated in Table I for the $q > \lambda$ and $k < \lambda$ region of the SRG unitary transformations for several different potentials, each evolved to $\lambda = 2$ fm^{-1}. That is, the SVD is applied to the matrix obtained when elements of $U_\lambda(k,q)$ with $k > \Lambda$ and $q < \Lambda$ are set to zero; in practice a cutoff $\Lambda \approx 2.5$ fm^{-1} is used to ensure that we are in the region where off-diagonal coupling is strongly suppressed everywhere in the Hamiltonian. The dominance of d_1 in each case is promising.

To test if a truncated outer product sum is a good approximation to the contribution from $k < \Lambda$, $q > \Lambda$, we consider the errors in some representative expectation values in Table II for several levels of truncation. The "zeroth-order" contribution is from the matrix where $k > \Lambda$ and $q > \Lambda$ is set to zero (this is denoted by SVD=0 in the table). The first-order (SVD=1 in the table) contribution uses the same matrix plus the approximation of $U_\lambda(k,q)$ for $k < \Lambda$ and $q > \Lambda$ given by the first outer product in the SVD expansion. The second order approximation uses two outer products, etc. The occupation and charge form factor operators shown here are chosen to illustrate the effects of the factorized approximation at

	SRG $\lambda = 1.5\,\mathrm{fm}^{-1}$				SRG $\lambda = 3.0\,\mathrm{fm}^{-1}$			
Operator	SVD	$q = 0.34$	$q = 3.01$	$q = 6.90$	SVD	$q = 0.34$	$q = 3.01$	$q = 6.90$
$\langle a_q^\dagger\, a_q \rangle$	0	7.61×10^{-7}	1.00		0	1.06×10^{-3}	1.00	
with N^{3}LO	1	7.61×10^{-7}	4.28×10^{-3}		1	1.06×10^{-3}	6.36×10^{-1}	
	2	7.61×10^{-7}	4.79×10^{-4}		2	1.06×10^{-3}	6.35×10^{-1}	
$G_\mathrm{C}(q)$	0	6.90×10^{-4}	5.01×10^{-3}	8.93×10^{-1}	0	4.10×10^{-4}	3.36×10^{-3}	8.92×10^{-1}
with NNLO	1	1.28×10^{-7}	8.90×10^{-5}	4.06×10^{-2}	1	1.63×10^{-4}	2.66×10^{-4}	4.00×10^{-1}
	2	1.04×10^{-6}	2.10×10^{-5}	4.18×10^{-2}	2	1.63×10^{-4}	3.04×10^{-4}	4.09×10^{-1}

TABLE II. Relative error of evolved operator matrix elements calculated using the SVD to factorize $U_\lambda(k,q)$ in the region where $k < \Lambda$ and $q > \Lambda$ (see discussion in text; units in fm^{-1}).

various momenta. Additionally, the initial occupation operator has no off-diagonal strength, whereas the initial charge form-factor operators have relatively substantial off-diagonal contributions at large values of q; this is significant for the applicability of factorization to an operator, as we see below. So, what we find at low momentum for the occupation operator is that it is essentially exact, up to errors resulting from decoupling and truncation of the wave function, and it is the same with or without the SVD approximation. This error increases, as expected, for larger λ. Because G_C is more diffuse initially, we see a small improvement even at small momenta when using the SVD approximations.

For the occupation operator at high momenta (well above the cutoff), the error is 100% without an approximation to $U_\lambda(k,q)$ because there is a hard cutoff and the initial operator is localized in the upper region of momentum space. However, with just one term in the SVD expansion we recover that expectation value for $\lambda = 1.5\,\mathrm{fm}^{-1}$ to better than 1%, and the situation improves with additional terms in the expansion. At $\lambda = 3.0\,\mathrm{fm}^{-1}$ decoupling is evidently not sufficient for this approximation to work well. At very large values of momenta (e.g., $q \approx 6.9\,\mathrm{fm}^{-1}$) the charge form factor shows improvement with the SVD approximation, but because this operator has significant off-diagonal strength, the improvement is not as pronounced. At a value of $q \approx 3.0\,\mathrm{fm}^{-1}$ it is evident that the SVD still improves the relative error. However, recall that the strength in the form factors is larger around $\approx \frac{1}{2}q$.

B. Connection to the Operator Product Expansion

The OPE was developed for the evaluation of singular products of local field operators at small separation. In our case, where such operators are treated as matrices and we typically work in momentum representation, the focus becomes low-momentum matrix elements of a product in which high-momentum states dominate the intermediate sum. This leads us directly to consider low- to high-momentum matrix elements of SRG-evolved operators, and a generic analysis is then based on the study of $U_\lambda(k,q)$ for $k < \lambda$ and $q \gg \lambda$.

The utility of the OPE rests on factorization; short-distance details decouple from long-distance dynamics. Factorization enables one, for example, to separate the momentum and distance scales in hard-scattering processes in terms of perturbative QCD and parton distribution functions. In our case, factorization is the direct result of decoupling. It provides tools that let us parametrize the high-momentum components of operators that would normally require degrees of freedom we do not retain. We can, for example, build effective

few-body operators containing state-independent functions of high momenta that can be measured directly in few-body experiments. These operators can then be employed to make predictions for A-body systems.

Consider a generic operator, $\widehat{O}_\lambda = U_\lambda \widehat{O} U_\lambda^\dagger$, and employ the spectral representation for U_λ:

$$U_\lambda(k,q) = \sum_\alpha \langle k|\psi_\alpha(\lambda)\rangle\langle\psi_\alpha(\infty)|q\rangle. \tag{4}$$

The OPE deals with cases in which the unevolved operator is dominated by high momenta (e.g., $a_q^\dagger a_q$ with large q is the simplest paradigm) and we focus on $k < \lambda$ and $q \gg \lambda$. For $k < \lambda$ we exploit the fact that low-momentum components of high-energy eigenstates of H_λ are exponentially suppressed because of decoupling. As a result the sum is dominated by low-energy states,

$$U_\lambda(k,q) \approx \sum_{E_\alpha \ll \lambda^2} \langle k|\psi_\alpha(\lambda)\rangle\langle\psi_\alpha(\infty)|q\rangle. \tag{5}$$

Once the sum is restricted we can turn our focus to approximating the high-momentum components of the unevolved low-energy states. This analysis is closely related to Lepage's discussion of the OPE analysis of wave functions, which leads him to write for S-waves in position representation [1]:

$$\Psi_{\rm true}(r) = \overline{\gamma}(r) \int d^3r\, \Psi_{\rm eff}\delta_a^3(\boldsymbol{r}) + \overline{\eta}(r)a^2 \int d^3r\, \Psi_{\rm eff}\nabla^2\delta_a^3(\boldsymbol{r}) + \mathcal{O}(a^4)\,, \tag{6}$$

where the coefficient functions $\overline{\gamma}(r)$ and $\overline{\eta}(r)$ are state-independent parametrizations of the short-distance physics, and a is approximately the distance of the ultraviolet cutoff. In this section, we outline how SRG factorization can be understood more generally (and analytically) in the context of the OPE for nonrelativistic Schrödinger problems by deriving an analogous equation in momentum space for the SRG-evolved wave function.

To do so, we first define the projection operators

$$\mathcal{P}_\Lambda = \int_0^\Lambda d\tilde{p}\ |p\rangle\langle p| \tag{7}$$

and

$$\mathcal{Q}_\Lambda = \int_\Lambda^\infty d\tilde{q}\ |q\rangle\langle q|\,, \tag{8}$$

where Λ divides momentum space and $d\tilde{p} \equiv \frac{2}{\pi}p^2\,dp$ in the partial-wave momentum basis. This Λ is to be distinguished from λ, which is the SRG evolution parameter and an approximate measure of decoupling in the evolved potential. We use ψ_α^λ to denote the eigenstates of the Hamiltonian ordered according to increasing energy E_α and evolved to λ via the SRG. H_λ and V_λ represent the corresponding SRG evolved Hamiltonian and potential. The initial, unevolved operators correspond to $\lambda = \infty$.

From the unevolved Schrödinger equation

$$H_\infty\,|\psi_\alpha^\infty\rangle = E_\alpha\,|\psi_\alpha^\infty\rangle\ , \tag{9}$$

we can write

$$\begin{pmatrix} \mathcal{P}_\Lambda H_\infty \mathcal{P}_\Lambda & \mathcal{P}_\Lambda H_\infty \mathcal{Q}_\Lambda \\ \mathcal{Q}_\Lambda H_\infty \mathcal{P}_\Lambda & \mathcal{Q}_\Lambda H_\infty \mathcal{Q}_\Lambda \end{pmatrix} \begin{pmatrix} \mathcal{P}_\Lambda \psi_\alpha^\infty \\ \mathcal{Q}_\Lambda \psi_\alpha^\infty \end{pmatrix} = E_\alpha \begin{pmatrix} \mathcal{P}_\Lambda \psi_\alpha^\infty \\ \mathcal{Q}_\Lambda \psi_\alpha^\infty \end{pmatrix}\ , \tag{10}$$

and thus for the "$\mathcal{Q}$" space we have

$$\begin{aligned}\mathcal{Q}_\Lambda \left|\psi_\alpha^\infty\right\rangle &= (E_\alpha - \mathcal{Q}_\Lambda H_\infty \mathcal{Q}_\Lambda)^{-1} \mathcal{Q}_\Lambda H_\infty \mathcal{P}_\Lambda \mathcal{P}_\Lambda \left|\psi_\alpha^\infty\right\rangle \\ &= (E_\alpha - \mathcal{Q}_\Lambda H_\infty \mathcal{Q}_\Lambda)^{-1} \mathcal{Q}_\Lambda V_\infty \mathcal{P}_\Lambda \left|\psi_\alpha^\infty\right\rangle \ , \end{aligned} \tag{11}$$

where we have used $(\mathcal{P}_\Lambda)^2 = \mathcal{P}_\Lambda$, $H_\infty = T + V_\infty$, and $\mathcal{Q}_\Lambda T \mathcal{P}_\Lambda = 0$. For low-energy states ψ_α^∞ such that $|E_\alpha| \ll \mathrm{Min}[|E_{\mathcal{Q}H\mathcal{Q}}|]$ (where $E_{\mathcal{Q}H\mathcal{Q}}$ are the eigenvalues of $\mathcal{Q}H\mathcal{Q}$), we can neglect the E_α dependence. Also, assuming that the potential $V_\infty(q', p)$ is slowly varying with respect to p compared to $\psi_\alpha^\infty(p)$ in the region $p < \Lambda$ and $q' \gg \Lambda$, we can use the expansion for S-waves

$$\begin{aligned}\int_0^\Lambda d\tilde{p}\, V_\infty(q', p)\psi_\alpha^\infty(p) \approx V_\infty(q', p')|_{p'=0} \times \int_0^\Lambda d\tilde{p}\, \psi_\alpha^\infty(p) \\ + \left.\frac{d^2}{dp'^2} V_\infty(q', p')\right|_{p'=0} \times \int_0^\Lambda d\tilde{p}\, p^2\, \psi_\alpha^\infty(p) \ + \cdots \end{aligned} \tag{12}$$

to first order, combined with the fact that the low-energy states will have momentum components peaked at small p, to write

$$\langle q|\psi_\alpha^\infty\rangle \approx -\int_\Lambda^\infty d\tilde{q}' \int_0^\Lambda d\tilde{p}\, \langle q| \frac{1}{\mathcal{Q}_\Lambda H_\infty \mathcal{Q}_\Lambda} |q'\rangle\, V_\infty(q', 0)\, \psi_\alpha^\infty(p) \ . \tag{13}$$

Tests indicate that these assumptions are valid for realistic NN potentials.

Further, we see empirically via Fig. **??** that $\mathcal{P}_\Lambda \left|\psi_\alpha^\infty\right\rangle \approx Z(\lambda) \left|\psi_\alpha^\lambda\right\rangle$ when $\lambda \gtrsim \Lambda$ (this is consistent with our understanding that the SRG with $G_s = T_{\rm rel}$ renormalizes/suppresses only the short-distance components of the wave function for values of λ considered here). Thus, setting $\Lambda = \lambda$ and defining

$$\gamma^\lambda(q) \equiv -\int_\lambda^\infty d\tilde{q}' \ \langle q| \frac{1}{\mathcal{Q}_\lambda H_\infty \mathcal{Q}_\lambda} |q'\rangle\, V_\infty(q', 0) \ , \tag{14}$$

we have

$$\psi_\alpha^\infty(q) \approx \gamma^\lambda(q) \int_0^\lambda d\tilde{p}\, Z(\lambda) \psi_\alpha^\lambda(p) \ . \tag{15}$$

So we see that the high-momentum components of low-energy eigenstates can be factorized into a state-independent function $\gamma^\lambda(q)$, which summarizes the short distance behavior of the wave function, and a coefficient (given by an integral over the renormalized wave function) that gives the contribution due to the long-distance structure of the state. Moreover, if we include higher-order corrections resulting from the expansion of $\int_0^\lambda d\tilde{p}\, V_\infty(q', p)\psi_\alpha^\infty(p)$ about $p = 0$, we recover the analog to Lepage's OPE, Eq. (6), in momentum space for the short-distance structure of a wave function. It is given by

$$\psi_\alpha^\infty(q) \approx \ \gamma^\lambda(q) \int_0^\lambda d\tilde{p}\, Z(\lambda) \psi_\alpha^\lambda(p) + \eta^\lambda(q) \int_0^\lambda d\tilde{p}\, p^2\, Z(\lambda)\, \psi_\alpha^\lambda(p) + \cdots \tag{16}$$

where $\gamma^\lambda(q)$ is given previously and

$$\eta^\lambda(q) \equiv -\int_\lambda^\infty d\tilde{q}' \ \langle q| \frac{1}{\mathcal{Q}_\lambda H_\infty \mathcal{Q}_\lambda} |q'\rangle \ \left.\frac{\partial^2}{\partial p^2} V_\infty(q', p)\right|_{p=0} \ . \tag{17}$$

Now, from the definition of the SRG unitary evolution operator in Eq. (**??**), in the region $k < \lambda$ and $q \gg \lambda$ we can use the leading-order term of our OPE to write

$$\begin{aligned} U_\lambda(k,q) &= \sum_\alpha^\infty \left\langle k|\psi_\alpha^\lambda\right\rangle \left\langle \psi_\alpha^\infty|q\right\rangle \\ &\approx \left[\sum_\alpha^{|E_\alpha|\ll|E_{\mathcal{Q}H\mathcal{Q}}|} \left\langle k|\psi_\alpha^\lambda\right\rangle \int_0^\lambda d\tilde{p}\, Z(\lambda)\psi_\alpha^{\lambda\dagger}(p)\right]\gamma^\lambda(q) \\ &\equiv K_\lambda(k)Q_\lambda(q)\ , \end{aligned} \tag{18}$$

where the sum is only over states in the "$\mathcal{P}$" space thanks to decoupling. Thus, we can understand the factorization of U_λ as a general consequence of our ability to factorize the high-momentum components of low-energy nuclear wave functions via an OPE plus decoupling in the SRG-evolved Hamiltonian. Moreover, because $\psi_\alpha^\lambda(k)$ to good approximation has no support when $k < \lambda$ for α in the "$\mathcal{Q}$" space, we can extend the α sum in Eq. (18) to the full space and apply closure to find

$$U_\lambda(k,q) \approx \left[Z(\lambda)\int_0^\lambda d\tilde{p}\sum_\alpha^\infty \left\langle k|\psi_\alpha^\lambda\right\rangle\left\langle\psi_\alpha^\lambda|p\right\rangle\right]\gamma^\lambda(q) \approx Z(\lambda)\gamma^\lambda(q)\ . \tag{19}$$

Thus, to a first approximation, $K_\lambda(k)$ is a constant factor.

This approximate constancy implies that the ratios for the $L = 0$ channels in Figs. 1(a) and 2(a) and (b) should tend to one in the factorization region, which is realized at the 10–20% level for sufficiently low λ. For $L > 0$, the generalization of Eq. (19) follows from modifying the Taylor series in Eq. (12) to account for $V_\infty(q',p) \propto p^L$ for small p. Then Eqs. (14) and (15) are changed to

$$\gamma^\lambda(q) \equiv -\int_\lambda^\infty d\tilde{q}'\ \langle q|\,\frac{1}{\mathcal{Q}_\lambda H_\infty \mathcal{Q}_\lambda}\,|q'\rangle\ \frac{d^L}{dp^L}V_\infty(q',p)\bigg|_{p=0}\ , \tag{20}$$

and

$$\psi_\alpha^\infty(q) \approx \gamma^\lambda(q)\int_0^\lambda d\tilde{p}\, Z(\lambda)p^L\psi_\alpha^\lambda(p)\ . \tag{21}$$

With these changes, Eq. (19) for the factorization at leading approximation becomes

$$U_\lambda(k,q) \approx \left[Z(\lambda)\int_0^\lambda p^L d\tilde{p}\sum_\alpha^\infty \left\langle k|\psi_\alpha^\lambda\right\rangle\left\langle\psi_\alpha^\lambda|p\right\rangle\right]\gamma^\lambda(q) \approx k^L Z(\lambda)\gamma^\lambda(q)\ . \tag{22}$$

This approximation implies that the ratios in the factorization region should tend for $L > 0$ to $(k_i/k_0)^L$, which is seen at the same 10–20% level in Fig. 1(b).

To gain insight into the implications of this factorization, we consider the expectation value of $a_q^\dagger a_q$ in a low-energy state, the deuteron. Because we know that strength in the evolved number operator expectation value decouples from high-momentum contributions in the deuteron, we can write

$$\begin{aligned} \left\langle\psi_d^\lambda\right|\left(a_q^\dagger a_q\right)_\lambda\left|\psi_d^\lambda\right\rangle &= \left\langle\psi_d^\lambda\right|U_\lambda\left(a_q^\dagger a_q\right)U_\lambda^\dagger\left|\psi_d^\lambda\right\rangle \\ &\approx \int_0^\lambda d\tilde{k}'\int_0^\infty d\tilde{q}'\int_0^\infty d\tilde{q}''\int_0^\lambda d\tilde{k}\,\psi_d^{\lambda\dagger}(k')U_\lambda(k',q')\delta(q'-q)\delta(q''-q')U_\lambda(q'',k)\psi_d^\lambda(k) \\ &= \int_0^\lambda d\tilde{k}'\int_0^\lambda d\tilde{k}\ \psi_d^{\lambda\dagger}(k')U_\lambda(k',q)U_\lambda(q,k)\psi_d^\lambda(k). \end{aligned} \tag{23}$$

For a low-momentum operator, one with $q < \lambda$, the expectation value thus depends only on the low-momentum details of the wave function (original and evolved). For $q \gg \lambda$, however, we can make use of factorization and set $U(k,q) \to K_\lambda(k) Q_\lambda(q)$ to write

$$\int_0^\lambda d\tilde{k'} \int_0^\lambda d\tilde{k}\, \psi_d^{\lambda\dagger}(k') K_\lambda(k') [Q_\lambda(q) Q_\lambda(q)] K_\lambda(k) \psi_d^\lambda(k) \tag{24}$$

from Eq. (23). Here we see that the expectation value of a high-momentum number operator is independent of the long-distance structure of the wave function. This is consistent with earlier calculations of the deuteron momentum distribution [4]. Again, as with decoupling in the potential, we appear to have a means by which long- and short-distance details can be separated for an operator evolved via the SRG.

The generalization of this result is straightforward. Consider the expectation value of an arbitrary operator, $O(q',q)$, in a low-energy state, $\psi_{\rm low}^\lambda$. Because decoupling is valid for operator expectation values in a momentum basis (as we have seen via the expectation value integrand plots in Secs. **??** and **??**), we can write

$$\left\langle \psi_{\rm low}^\lambda \right| U_\lambda \widehat{O}\, U_\lambda^\dagger \left| \psi_{\rm low}^\lambda \right\rangle \approx \int_0^\lambda d\tilde{k'} \int_0^\infty d\tilde{q'} \int_0^\infty d\tilde{q} \int_0^\lambda d\tilde{k}\, [\psi_{\rm low}^\lambda(k')]^\dagger U_\lambda(k',q') O(q',q) U_\lambda(q,k) \psi_{\rm low}^\lambda(k) \,. \tag{25}$$

We separate the integrals over the operator in the expectation value and apply factorization to set $U(k,q) \to K_\lambda(k) Q_\lambda(q)$ in the region where $k < \lambda$ and $q \gg \lambda$. If the *unevolved* operator has coupling between high and low momentum above the the factorization cut, then there is no great simplification. However, if the *unevolved* operator *does not* have coupling of high and low momentum above the factorization cut, factorization will allow us to separate out the high- and low-momentum structure of an operator into two contributions:

$$\int_0^\lambda d\tilde{k'} \int_0^\lambda d\tilde{q'} \int_0^\lambda d\tilde{q} \int_0^\lambda d\tilde{k}\, [\psi_{\rm low}^\lambda(k')]^\dagger U_\lambda(k',q') O(q',q) U_\lambda(q,k) \psi_{\rm low}^\lambda(k) \tag{26}$$

and

$$\int_0^\lambda d\tilde{k'} \int_\lambda^\infty d\tilde{q'} \int_\lambda^\infty d\tilde{q} \int_0^\lambda d\tilde{k}\, [\psi_{\rm low}^\lambda(k')]^\dagger K_\lambda(k') [Q_\lambda(q') O(q',q) Q_\lambda(q)] K_\lambda(k) \psi_{\rm low}^\lambda(k) \,. \tag{27}$$

This is analogous to what was found for the number operator.

Thus, we see that the breakdown of contributions to the expectation value of a general operator is consistent with our interpretation of the SRG flow equations as a means by which one can achieve a separation of scales in the evaluation of nuclear few- and many-body problems. We see explicitly here that the effects of a low-momentum probe of the ground state wave function depends (almost entirely) on the low-momentum details of the renormalized wave function. Likewise, the effect of a high-momentum probe is largely independent of the low-momentum structure. It is only for operators which probe the coupling of high and low momentum (long and short distance) details of the wave function that we must consider the full momentum space evolution of the operator. For the operators that have been considered in this paper, the latter is only true of the electromagnetic form factors at relatively high momenta (beyond the typical regime of interest for nuclear structure); for any operators which weakly couple high and low momentum, these terms can be neglected.

To summarize, we can write the expectation value of an operator that has weak coupling between high and low momentum as

$$\left\langle \psi^{\lambda}_{\rm low} \right| U_\lambda \widehat{O}\, U^\dagger_\lambda \left| \psi^{\lambda}_{\rm low} \right\rangle \approx \int_0^\lambda d\tilde{k}' \int_0^\lambda d\tilde{k}\, [\psi^{\lambda}_{\rm low}(k')]^\dagger \Big[\int_0^\lambda d\tilde{q}' \int_0^\lambda d\tilde{q} \times U_\lambda(k',q') O(q',q) U_\lambda(q,k) + I_{QOQ} K_\lambda(k') K_\lambda(k) \Big] \psi^{\lambda}_{\rm low}(k) \ , \quad (28)$$

where

$$I_{QOQ} = \int_\lambda^\infty d\tilde{q}' \int_\lambda^\infty d\tilde{q}\ Q_\lambda(q') O(q',q) Q_\lambda(q) \ . \quad (29)$$

By using factorization, we have seen that the expectation value breaks into a sum of two components: one which describes low-momentum structure, and a high-momentum component that factorizes into a piece depending on the low-momentum structure, and another piece that is a universal function of high momentum q.

III. NEW OR ADDITIONAL PLOTS

A. $L \geq 1$ partial waves

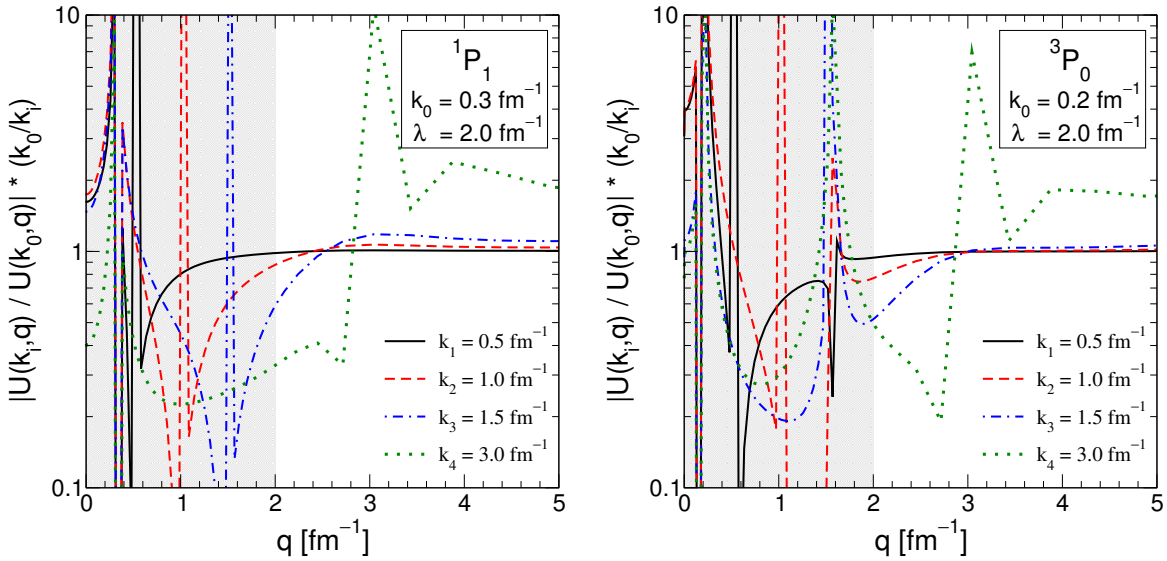

FIG. 3. Same as Fig. 1 but for the (a) ^{1}P$_1$ partial wave scaled and (b) ^{3}P$_0$ partial wave scaled, both at λ of 2.0 fm^{-1}.

From Eq. (22), factorization at leading approximation for a partial wave with orbital angular momentum L,

$$U_\lambda(k,q) \approx k^L Z(\lambda) \gamma^\lambda(q) \ , \quad (30)$$

so the normalized ratio

$$\left(\frac{k_0}{k_i}\right)^L \frac{U_\lambda(k_i,q)}{U_\lambda(k_0,q)} \approx 1 \ . \quad (31)$$

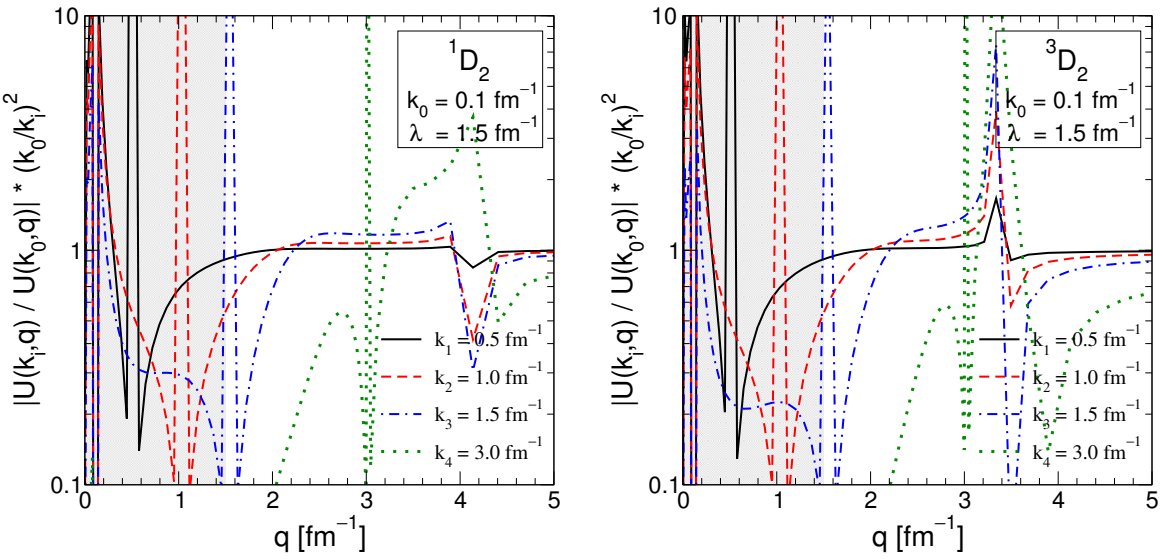

FIG. 4. Same as Fig. 1 but for the (a) $^1D_2$ partial wave scaled and (b) $^3P_2$ partial wave scaled, both at λ of 1.5 fm^{-1}.

in the factorization region. This was roughly apparent for $^1P_1$ in Fig. 1(b), but we show more examples here in Figs. 3 and 4. Comments:

- The scaled P-waves in Fig. 3 show similar behavior for the ratios as the S-waves did. The ratio $^3P_0$ happens to be a bit more uniform at one for $q \geq 3\,\mathrm{fm}^{-1}$, and as k_i gets closer to λ
- Note that for these calculations the mesh is quite coarse in the region of 3 to 5 fm^{-1}, where there are only eleven points, most of them near 3 fm^{-1}.
- The D-waves in Fig. 3 don't seem to work as well as the S-waves and P-waves. In particular, there are some problems around particular points. However, this happens when the denominator becomes very small (because we take the absolute value, this is presumably near where it goes through zero). With the coarseness of the grid, just issues with numerical precision would account for the deviations of the ratio from unity. We can check this by re-running with a grid more appropriate for that region.

[1] G. Lepage, in *Lectures given at 9th Jorge Andre Swieca Summer School: Particles and Fields, Sao Paulo, Brazil* (1997), nucl-th/9706029.

[2] E. Braaten and L. Platter, Phys. Rev. Lett. **100**, 205301 (2008), arXiv:0803.1125.

[3] R. B. Wiringa, V. G. J. Stoks, and R. Schiavilla, Phys. Rev. C **51**, 38 (1995), nucl-th/9408016.

[4] S. K. Bogner, R. J. Furnstahl, R. J. Perry, and A. Schwenk, Phys. Lett. B **649**, 488 (2007), nucl-th/0701013.

[5] L. Frankfurt, M. Sargsian, and M. Strikman, Int. J. Mod. Phys. A **23**, 2991 (2008), arXiv:0806.4412.

[6] S. C. Pieper, R. B. Wiringa, and V. R. Pandharipande, Phys. Rev. **C46**, 1741 (1992).
[7] E. D. Jurgenson and R. J. Furnstahl, Nucl. Phys. A **818**, 152 (2009), arXiv:0809.4199.
[8] E. Anderson, E. J. Jurgenson, R. J. Furnstahl, , and R. J. Perry (2010), in preparation.